Higher Order Sectorization in LTE Downlink with 3GPP Release 10 Closed Loop MIMO Transmission Techniques

Le Hang Nguyen and Andreas Weber
Bell Laboratories, Nokia, Stuttgart, Germany
Email: {le_hang.nguyen, andreas.weber}@nokia-bell-labs.com

***Abstract*—An extensive evaluation on the system performance of a conventional LTE wide beam tri-sector site network exploiting 3GPP Rel. 10 advanced closed loop MIMO transmission techniques (CL-MIMO) with that of a Higher Order Sectorized (HOS) network has been carried out. The investigation emphasizes on a system performance assessment under realistic conditions. These include a real MCS link adaptation with HARQ processes, adaptive scheduling algorithms, standardized CL-MIMO with the corresponding feedback mechanism and antenna characteristics as parameterized by the antenna manufacturers. The fundamentals of HOS is first explained on the basis of a simple single transmit antenna system per sector. Then antenna diversity is introduced into the system. System performance comparison for a practical network with a fixed number of transmit antenna elements per site (24 Tx antenna elements/site) is carried out for various network layouts applying either MIMO and/or HOS. For the latter 2 variants of deployments are considered: hard-sectorization, where multiple antenna elements with narrower beam width are used to cover smaller sub-sectors and soft-sectorization, in which fixed beam forming by means of pre-coding weights applied on an antenna array is exploited for sector forming. Constraint to Rel. 10 feedback mechanism, numerical results indicate advantages in deploying HOS over CL-MIMO usage, provided that large antenna array with suitable pattern characteristics for forming virtual sectors are available.**

I. Introduction

When it is required to increase capacity the service providers have several options: to densify the network like done with HetNet and small cells or to use new spectrum. These are efficient but expensive responses. Massive MIMO is another altenative which promises huge gains but is still expensive. Another strategy is to maximize the capacity utilization of the existing spectrum in macro cell networks by practical techniques and efficient algorithms. As such, higher order sectorization (HOS) aims at spectrum reuse by splitting a sector in 2 or multiple sub-sectors. The following questions are raised: how much from the expected spectrum reuse gain can be harvested in an *operational* network? Considering todays standard of multiple antenna element systems and the sophisticated standardized CL-MIMO, what are the most beneficial techniques to be deployed given a fixed number of transmit antenna elements per site in the network?

The HOS idea is already known in the UMTS/WCDMA standard and can be found in some standard works and publications [1], [2], [3]. In [4] the authors investigated the performance of a downlink LTE system when going from 3- to 6-sector sites in either horizontal or vertical direction for a large range of inter-site distances (ISD) for urban and rural scenarios. For the urban macro scenario an inhouse ray based statistical channel model is used for the simulation and for the rural scenario a simple path loss propagation model is considered. In [5] the authors compared the mean user throughput of a 12-sector site network equipped with single transmit antennas to the performance of a conventional 4Tx antenna tri-sector site network performing MU-MIMO techniques. Results were analytically obtained. As in most of the publications important features of an operational system like feedback and real MCS adaptation were also omitted in [4] and [5].

A typical application area for HOS is the interference limited urban macro scenario. We therefore concentrate our study on an LTE downlink system in an urban macro network. The study focuses on a system performance assessement under *realistic* conditions, i.e., we consider a practical MCS link adaptation with HARQ mechanism, limited and inaccurate feedback due to channel aging and quantization errors as well as the interplay between HOS and the 3GPP Rel. 10 facilitated CL-MIMO transmission techniques. Two realization approaches for HOS are considered: hard- and soft-sectorization. The first variant deploys antennas with narrower beamwidth to serve smaller sectors. The latter relies on antenna arrays to form fixed beam patterns which virtually define the sub-divided sectors.

This study is structured as follows: in the second section we summarize the parameter settings and the main features of the simulation tools used for this study. On the basis of a simple system with single transmit antenna element per sector we will then briefly demonstrate some important relations between HOS gain and simulation conditions. In the next section we introduce antenna diversity into the system. For a fixed number of 24 transmit antenna elements per site (8Tx per tri-sector cell) a performance comparison for a conventional tri-sector site and a HOS network considering advanced CL-MIMO transmission techniques defined in 3GPP Rel.10 will be shown.

II. Parameter settings and simulation tool

For the numerical study we used a 3GPP LTE Rel.10 compliant simulation tool. A wrap-around hexagonal network is considered. An average number of 30 users per site is randomly dropped at the beginning of each batch and kept the same for all network layouts under investigation i.e. in average 10 users per cell in a standard tri-sector site and 5 users per cell in a 6-sector site network configuration are generated. Each simulation is carried out with 5 batches, each lasts 1s (1000 transmission time intervalls). A geometry-stochastic based 2D spatial channel model, the 3GPP UMa model [6], was used. Fast fading, path loss and shadowing are considered. For the purpose of angular spread of departure (ASD) dependency investigation we varied the 3GPP defined ASD (23°) over a range of values. The final results were obtained for an ASD of 8°. Instead of the defined 30 km/h a 3 km/h speed was chosen to emulate a pedestrian scenario. Other parameters are essentially the same as the typical 3GPP settings for an urban macro scenario. A 3D parabolic antenna pattern has been used based on the analytic formula defined by 3GPP [7]. Feedback delays and quantizations for a real MCS link adaptation are taken into account. The terminal antenna is equipped with 2 omni-directional co-polarized elements at a height of 1.5 m. Full buffer traffic was assumed.

A. The MU-MIMO scheduler

The MU-MIMO scheduler is based on the proportional fair (PF) scheduler which optimized the weighted sum rate. Scheduling decisions are done per user and per scheduled resource unit. A greedy algorithm is used for the user pairing mechanism. Starting with the highest priority user a set of active users potentially suited for co-scheduling is pre-selected according to a pre-defined channel correlation threshold. The scheduler succesively adds co-scheduled users, which improve the total cell throughput. It stops searching for further co-scheduled users as soon as the currently selected candidate contributes no improvement to the total system throughput. For predicting the system throughput, signal-to-leakage and noise ratio (SLNR) based transmission precodings are used [8]. Note that, unlike as assumed in most publications, e.g. [9], the LTE CQI feedback does not contain the channel matrix, but only the precoding matrix identifier (PMI) which can be transformed into an equivalent MISO channel [10]. The total transmit power is equally divided among all co-scheduled users but the transmit power does not need to be equally divided over all individual antenna elements.

B. 3D antenna beam pattern

The approximated 3D antenna beam is modelled by the azimuth and vertical parabolic pattern cuts according to 3GPP [7]. The parabolic pattern is parametrized by the Half Power Beam Width (HPBW) and the Front-to-Back Ratio or in the vertical direction the Side Lobe Level (SLL). These parameters are summarized in table I and are taken from data sheets specified by Kathrein [11] .

Figure 1 exemplarily shows a measured (solid) and an approximated (dotted) parabolic antenna pattern. The approximation describes well the main characteristics of the antenna beam pattern. The sidelobe is averaged by a constant offset floor.

[2] http://www.kathrein.de/en/mobile-communication/portal/radiation-patterns-for-mobile-communication-antennas

Antenna type HPBW	742351v01 33°	742218 44°	80010504 64°
Maximal Gain [dB]	20.7	19.5	17.7
vertical HPBW [dB]	7.2	6.8	6.7
vert. SLL [dB]	>18	> 18	>16
Horz. front-to-back ratio [dB]	30	30	25

Table I
ANTENNA PARAMETERS USED IN THIS STUDY. THEY ARE TAKEN FROM KATHREIN'S TECHNICAL SHEETS [11].

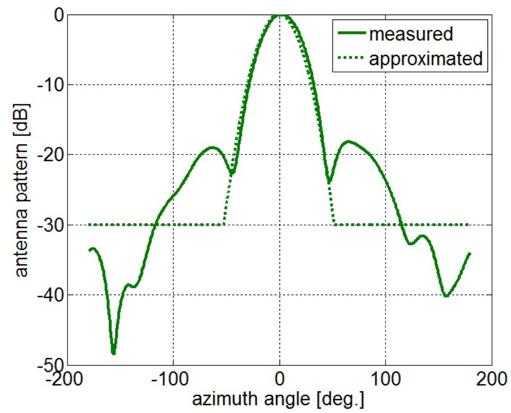

Figure 1. The approximated (dotted) parabolic pattern using parameters specified in Table I and the measured (solid) antenna pattern [2] in the azimuth direction (Kathrein Type 742351v01).

III. NETWORK WITH SINGLE TRANSMIT ANTENNA ELEMENT PER SECTOR: FACTORS IMPACTING SECTOR SPLITTING GAINS

By splitting gain we mean the performance gain obtained when each sector is split into 2 or multiple sub-sectors. Each of these sub-sectors transmits with the same number of antenna elements and uses the same power as the original sector to serve the same total number of users in a site as before (the number of users per site is kept constant). It is theoretically expected that the splitting gain should then scale with the number of the sub-sectors due to spatial reuse, larger number of transmit antenna elements and power. In praxis inter-sector interference due to sector overlapping and channel angular spreading limits the achievable gain. Further, applying other sophisticated algorithms like PF (also MU-MIMO) scheduling exploits the spatial system diversity (in the sense that it preferably schedules users during good channel conditions, i.e. when the expected throughput is higher than the average obtained throughput). Deploying sub-sectorization in combination with these techniques can only harvest the left-over diversity for spatial reuse gain. Hence the splitting gain also depends on the performance of the applied scheduling

algorithms in the networks.
In order to illustrate the 3 mentioned possible impact factors: the sector beam pattern, the channel angular spread and the applied scheduling mechanism, we consider a simple macro network with base stations employing single antenna element and standard proportional fair scheduler.

A. Impact of the antenna beam pattern

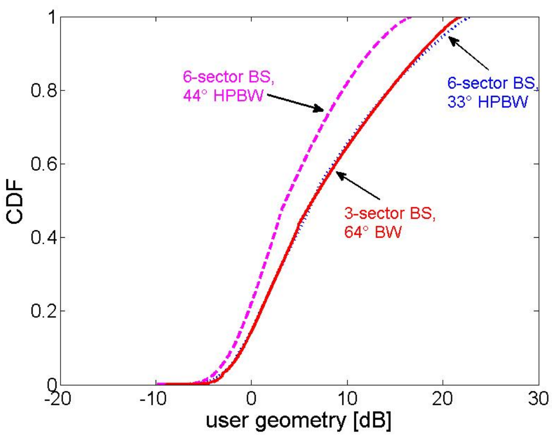

Figure 2. User geometry distibution for a traditional tri-sector site network with 64° HPBW (solid red) and 6 sector site network using antennas with with 33° HPBW (dotted blue) 44° HPBW (dashed magenta). The parameters for the applied antennas are summarized in table I. The red and blue curves are nearly identical. This suggests a doubling in system throughput when switching from 3 to 6 sector site network using the 33° HPBW antennas.

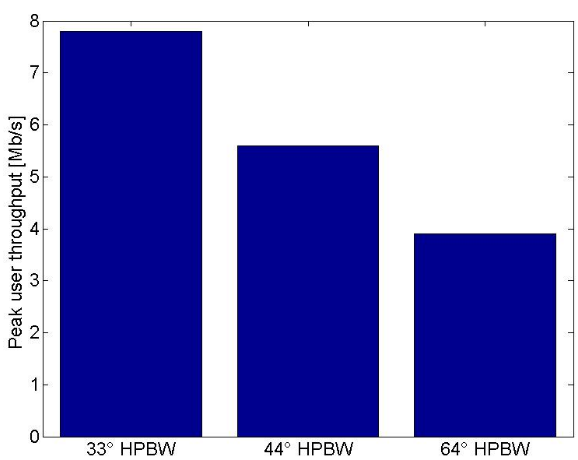

Figure 3. Peak user throughput (95% point of the user throughput CDF) for the different network layouts. It doubles as the sector number doubles provided that the beamwidth is properly scaled.

The beam shape is critical to sector splitting gain. Antennas perfectly suited for sub-sectorization would deliever a rectangular shape response, which is confined within and equal to zeros outside the sub-sectors. Any leakage beyond the sector border (as in parabolic case) leads to interference. Sector pattern characteristics are optimized by antenna manufacteurs using reflectors and housing amongst others. In soft sectorization case array layout and filter design determine the sub sectorization performance.
Fig. 2 shows the user geometry distribution for tri (solid red) and 6-sector site networks. User geometry is defined as the average received wideband SINR of a user at a certain position in the cell. It depends on transmit power, antenna gain, distance dependent path loss, shadowing and the system thermal noise. Effects stemming from fast fading and scheduler can be excluded. Two types of narrow beam antennas, 44° (dashed magenta) or 33° (dotted blue) HPBW, are used for the realization of the 6-sector site networks. The front-to-back ratio defines the user geometry upper bound. The larger inter-sector overlapping when using 44° HPBW antennas leads to high interference and degrades the SINR compared to that in the conventional 3-sector site case. In contrast, when using antennas with 33° HPBW nearly identical SINR distribution compared to that of the conventional tri-sector system can be achieved (red and blue curves). Identical SINR with a double number of sectors per site would theoretically mean a doubling in the site throughput. Actually a doubling in the measured peak throughput (95% point of cumulative distribution function of the user throughput) for the higher order sectorized network using 33° HPBW antennas can be observed (cf. fig. 3). The difference at high SINR region originates from the following two opposing effects: the users close to BS with high SINR experience in the sub-sectorized configuration backward radiation coming from 5 instead of 2 intra-site interfering sectors. This increase in interference is the counterpart to the better front to back ratio of 30 dB for 33° compared to 25 dB for 64° HPBW antennas. In total an improvement of 1 dB in higher SINR region results for the 6 sector site case.

B. Impact of the channel characteristics

A realistic macro channel link is spread out by a number of direct and indirect paths which are determined by the surrounded scatterers. This scattering increases the effective overlapping regions between sectors and resulting in a stronger inter-sector interference. The smaller the sector area the higher is the related impacts on the system performance. Fig. 4 shows user mean (upper plot) and edge (lower plot) throughput as a function of the channel angular spread of departure. Stronger dependency of the edge compared to the mean user throughput and of HOS network configuration compared to conventional wide beam 3-sector site layout can be observed. The splitting gain in mean and edge user throughput varies between $(84-50)\%$ and $(65-0)\%$, respectively. The stronger dependency of the edge throughput on the angular spread is intuitive, since the interference due to the isolation loss between the adjacent sectors is especially severe for the low SINR edge users. Similar effect can be observed increasing the angular spread. The edge user throughput for the different layouts intersects each other at an angular spread of about 32. Extrapolating to larger angular spread, even a degradation of system throughput is expected for higher order network.

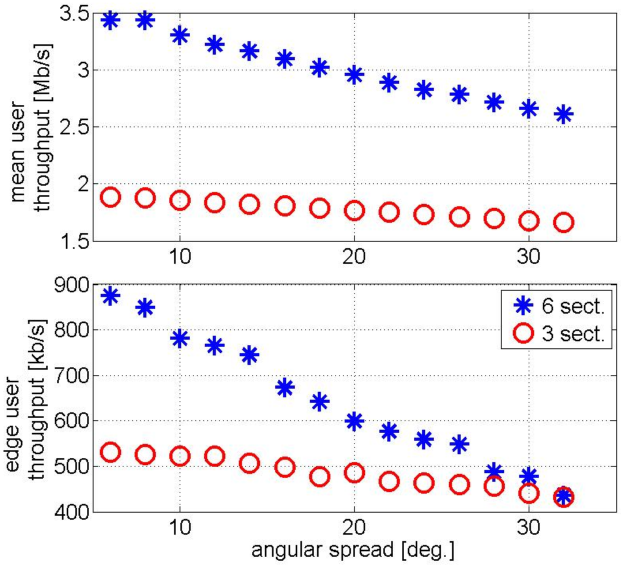

Figure 4. Mean (top), edge (bottom) user throughput as a function of the channel's azimuth angular spread of departure (ASD) for a conventional 3-sector and a 6-sector site network applying single transmit antenna elements (antenna height for BS = 25 m and terminal = 1.5 m). PF scheduler is used. A stronger dependency on the angular spread is observed for higher order sectorized configuration and for edge user throughput. Splitting gain varies between (84-50)% in mean and between (65-0)% in edge user throughput.

C. Impact of applied scheduling algorithms

Sophisticated scheduling algorithms can exploit diversity in the network and increase so the system performance. The Round Robin (RR) scheduler assigns the available resources to the scheduled user, one after the other. In contrast the PF scheduler selectively schedules the users at good channel conditions. In doing so it exploits already to a certain degree the system diversity. As a consequence there is less diversity left to be harvested compared to a system using a simple RR scheduler. Table II shows the mean, edge and peak user throughput (TP) for networks working with PF and RR scheduler in a macro environement with an ASD = 8°. An overall better performance for networks using PF than that applying RR schedulers can be observed. In contrast to this the splitting gain, as stated w.r.t. to the performance of the 3 sector system using the same scheduler type is lower for the case of PF scheduler.

	Mean TP [Mb/s]	Edge TP [kb/s]	Peak TP [Mb/s]
proportional fair			
3 sector site	1.88	526	4010
6 sector site	3.43	849	8560
Splitting gain	83%	61%	113%
round robin			
3 sector site	1.54	398	3480
6 sector site	2.93	677	7580
Splitting gain	91%	70%	118%

Table II
SECTOR SPLITTING GAIN FOR RR AND PF SCHEDULERS.

IV. HIGHER ORDER SECTORIZATION IN SYSTEMS WITH MULTIPLE ANTENNA ELEMENTS

We include now to the considered system multiple antenna elements. Since HOS performs best at small angular spread, as seen above, we restrict our investigation to an angular spread of 8° in an urban macro scenario. Release 10 defines MIMO precoding for up to 8 antennas. In the following section we will fix the number of antenna elements per site to 24, e.g. a 8Tx co-polarized (||||||||) or 4 pairs (XXXX) of cross-polarized antenna elements per cell in a conventional tri-sector network. Switching to a higher order 6-sector site configuration (hard-sectorization), each cell can then be equipped with 4 co-polarized (||||) or 2 pairs of cross-polarized antenna elements (XX). The orientation of the antenna array in this case is adapted to the sector configuration in the site such that the interference to sectors in adjacent sites is minimized. To each of these network layouts CL-MIMO can be applied. Adaptively to the channel conditions either single user (SU) and/or MU-modes are used. Another possible network configuration, the soft-sectorization, keeps the physical sector arrangement of the conventional tri-sector network and applies fix precodings to perform sector beam forming. In this way virtual soft-sectors can be defined, each equipped with virtual antenna elements, having its own cell ID and operating independently with its own scheduler. Figure 5 illustrates the different possible network realizations investigated in this study.

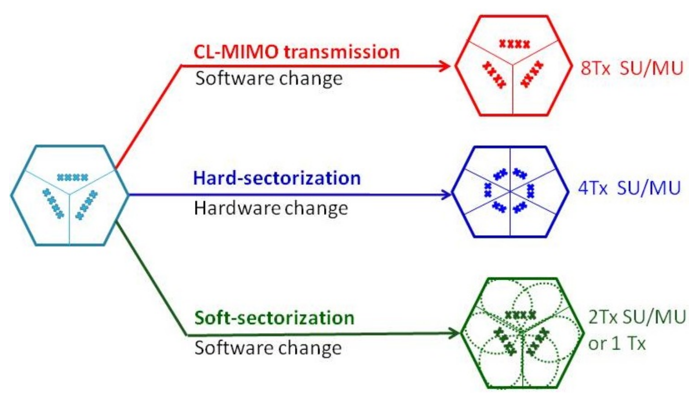

Figure 5. Different network realizations based on 12 pairs of cross polarized antenna elements (24 RF chains) per site: CL-MIMO transmission, hard- and soft-sectorization.

A. Hard-sectorization

We consider here the hard sectorization network layout as described above using a cross-polarized antenna array (XXXX). Antenna parameters of a 33° HPBW panel are used for the numerical investigation. The smaller coverage area of the higher order sector allows to use a larger antenna element spacing than the standard 0.5λ value commonly used for the conventional wide beam tri-sector network. This narrows the beam width in the MIMO operation and reduces so the interference. An inter-antenna elements spacing of 0.8λ is optimal for the considered hard-sectorized network.

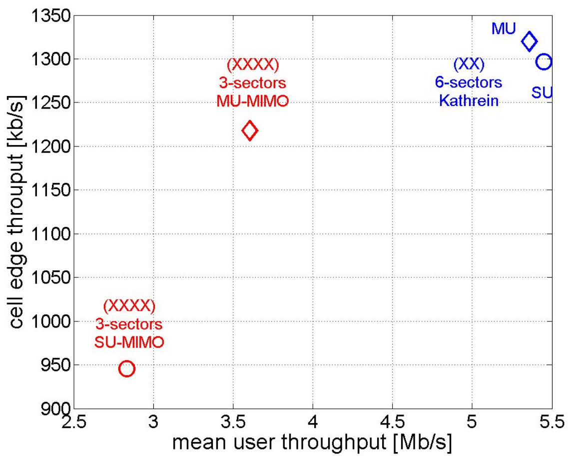

Figure 6. Hard-Sectorization based on (XXXX) system: mean and edge user throughput for different network configurations with 24 antenna elements per site. The total transmit power per site is kept constant. A spacing of d = 0.5λ (tri-sector) and 0.8λ (6-sector) is used.

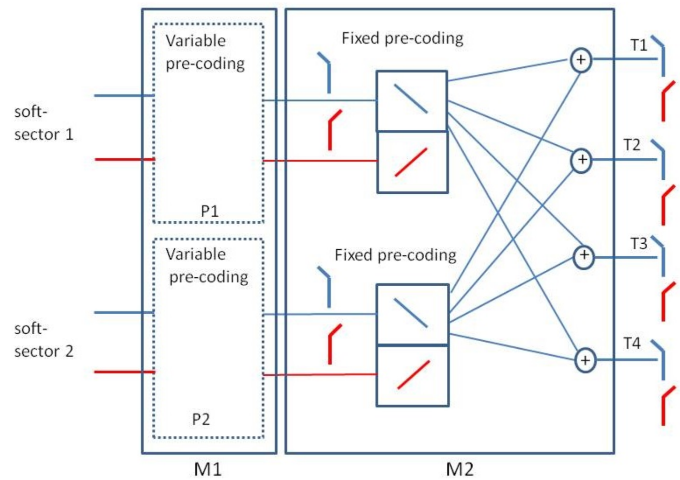

Figure 7. The concept of soft-sectorization is illustrated for a tri-sector network whose cells are equipped with 4 pairs of cross-polarized antenna elements (XXXX). The 4 pairs of antenna elements transmit with a total output power T_{total}. Each (hard)-sector is sub-divided into 2 soft-sectors formed by arrays of antenna elements with the same polarization. Each soft-sector transmits with a pair of virtual cross-polarized antenna elements. The sum output signal power at the virtual antenna of each soft-sector amounts to $T_{total}/2 = (T1 + T2 + T3 + T4)$.

Fig. 6 shows mean and edge user throughput for the tri-sector site network (red symbols) applying CL SU-MIMO (circle) and MU-MIMO (diamond) transmission techniques. Results for higher order hard-sectorized network are depicted in blue. Performance improvement in mean and edge user throughput up to 28% and 29% respectively can be observed when in the conventional tri-sector network MU-MIMO is deployed. This can be attributed to the fact that sharp beams can be formed with 8Tx, thus generating a high number of potential co-scheduled users for MU-MIMO pairing and to the better opportunity in a large sector area to spatially separate served users. In contrast to this in the higher order hard-sectorized network no improvement can be harvested from MU-MIMO deployment (blue symbols). The small reduction in the mean user throughput is offset by the gain in the edge user throughput and demonstrates the effect of the limited MIMO feedbacks on a real link adaptation. On the other hand when comparing with a conventional tri-sector network the higher order hard-sectorized network exhibits a largely higher performance, improved by 92% and 37% (w.r.t. performance of conventional tri-sector network) in mean and edge user throughput, respectively.

B. Soft-sectorization

In this section we first consider the performance of a soft-sectorized network using the cross-polarized setting (XXXX) as above. We will include latter the investigation for a co-polarization setting (||||||||). Fig 7 shows the schematic diagram of the signal flow for the soft-sectorized network. In each sector there are 2 sets of antenna elements with the same polarization available for the beam shaping. Each of these 2 antenna arrays is used to synthesize 2 beams by means of fixed precoding weights stearing the beams to $\pm 30°$ off the main direction of the physical sector. The 2 soft-sectors formed in that way are equipped with one pair of virtual cross-polarized antenna elements. So effectively one uses 4 antenna elements to form one sector beam. And therefore each input signal to the fixed precoder is distributed over the 4 antenna elements. Within the soft-sectors and according to the channel conditions of a scheduled user further variable pre-coding can be used. The total power of the conventional tri-sector cell is equally divided between the created soft-sectors. And each soft-sector is an individual virtual cell with its own cell ID. In constrast to hard-sectorization, the number of transmit antenna elements for the virtual soft-sectors is defined by the number of available different polarizations, since the whole array is used to form the virtual sectors. As observed in section IV-A limited MU-MIMO gain is expected when applying to system with less than 4 Tx (XX). We therefore consider in the case of soft-sectorization SU-MIMO only. The soft-sectorized system illustrated in Fig 7 can be described by

$$\mathbf{x} = \mathbf{M_2} * \mathbf{M_1} * \mathbf{s} \tag{1}$$

where $\mathbf{s}$ corresponds to the transmit signals at the virtual antennas of the soft-sectors 1 and 2, stacked in a [4x1] vector. $\mathbf{M_1}$ is a [4x4] diagonal matrix composed by the variable pre-codings $\mathbf{P_1}$ and $\mathbf{P_2}$ (see figure 7), as reported by the UEs in the soft-sectors 1 and 2. $\mathbf{M_2}$ is a [8x4] matrix containing the fix pre-codings determined the antenna weights to form the two soft-sector patterns. These fix pre-codings are designed such that the phase delays between array elements in the steered direction are compensated. x is a [8x1] vector of the pre-coded transmit signals at the physical antenna elements.

1) cross-polarized antenna array (XXXX): Important design criteria for soft-sectorization is the right trade-off between angular coverage of the created sector beams and the interference induced by inter-soft-sector overlapping. Using an uniform linear array to form and steer beams towards a certain direction one benefits from antenna array gain in the steered direction but at the same time interference is generated in other directions (other sector beams) due to the occuring sidelobes.

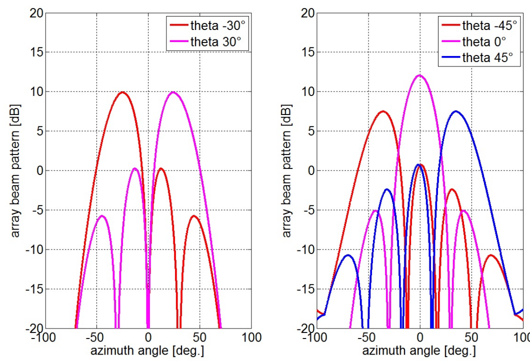

Figure 8. Angular coverage of soft-sector pattern gain for 2 (left) and 3 (right) soft-sectors, using a 4 element array.

The left plot in figure 8 shows such shaped beams using a 4 Tx element array. The beams are directed towards $\phi_\circ = \pm 30°$ (left plot). A coverage gap can be seen at $\phi = 0°$ as well as the interfering sidelobes in the adjacent beams. The coverage gap can be filled by a third soft-sector at the expense of increasing interference due to higher total sidelobe level and larger inter-soft-sector overlapping in coverage areas. The right plot in figure 8 illustrates the 3 soft-sectors whose main directions are pointed to $\phi_\circ = \pm 45°, 0°$.

There are means to suppress the array induced sidelobes for example the use of Dolph-Chebyshev filter. This applies an additional different real weights to the antenna elements which are normalized in such a way that the total transmit power is not changed. The applied power at each individual antenna element needs not to be the same. This put an additional constraint on the power amplifier performance. In addition to the interference reduction effect the Dolph-Chebyshev filter at the same time broadens the beamwidth, depending on the desired sidelobe level suppression. This beamwidth broadening can either be helpful in filling the coverage gap as demonstrated in the most upper plot of figure 9. On the other hand it generates additional interference due to the increasing overlapping of the adjacent soft-sectors. In general to get the benefits the applied filter has to be carefully designed. Depicted in the middle plot of figure 9 are the wideband SINR distribution of a 6 soft-sectorized network with (dotted green) and without (solid green) filter usage. Improvement associated to the utilization of Chebyshev taper can be observed. Comparing to hard-sectorized soft sectorized network applying Chebyshev filter exhibits similar SINR distribution. This suggests at the first glance a similar system performance. Unfortunately this is not the case as seen in the bottom plot of figure 9. It shows the mean and edge user throughput for the 3 considered network configurations.The system performance of the hard-sectorized network is much higher than that of other layouts. This becomes intuitively

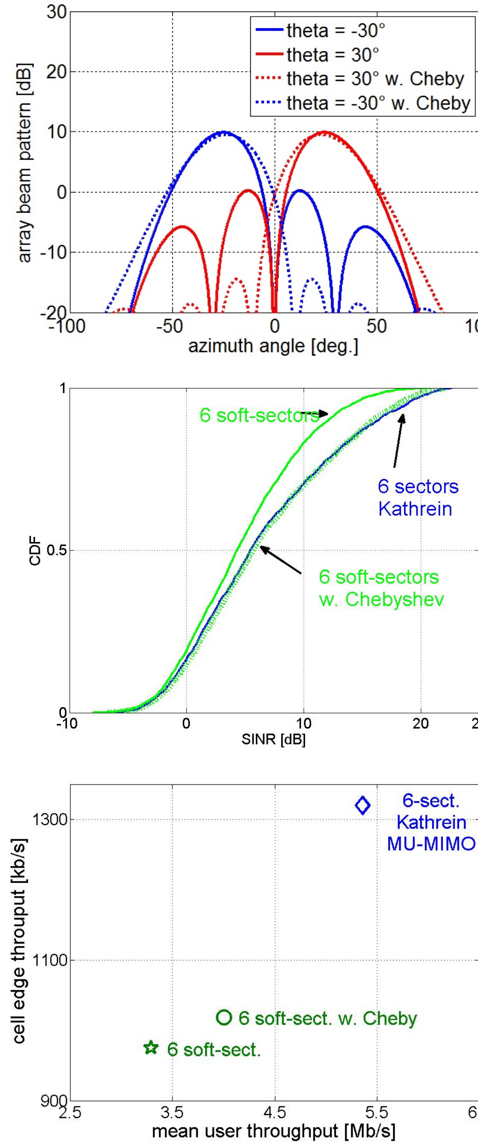

Figure 9. Top: beams formed by uniform progressive phase compensation weights (solid) and non-uniform Chebyshev weights (dotted) for a 4 element array. Filled coverage gap and sidelobe suppression can be observed. Middle: wideband SINR distributions for 6-sectorized network: hard (blue), soft (green solid) and soft with Chebyshev filter (green dotted). Significantly improvement in the SINR distribution associated with the usage of Dolph-Chebyshev filter can be observed. Soft-sectorized configuration using spatial Chebyshev filter exhibits similar SINR distribution as the 6 hard-sectorized network. Bottom: mean and edge user throughput for 6 soft-sectorized network (green star), 6 soft-sectorized network applying Chebyshev taper (green circle) and 6 hard-sectorized network using antenna elements with 33° beamwidth. The latter demonstrates the best performance.

clear considering the fact that the hard-sectors transmit with 4 Tx (XX), whereas the soft-sector counterparts operate with 2 virtual Tx (X) antenna elements only.

Figure 10 shows the mean and edge user throughput for various variants of network configurations based on a system using cross-polarized antenna arrays. Following network configurations are considered: conventional tri-sector (red) and 6 hard-sectorized (blue) network using SU-/MU-MIMO as well as 6 (green), 9 (purple), 12 (magenta) soft-sectorized networks, with and w/o Dolph Chebyshev taper. The 6 hard-sectorized configuration performs the best. Increasing the number of soft-sectors from 6 to 9 clearly improves the performance in both mean and edge user throughput, which associates with a better sector coverage as discussed above. Further increasing the number of soft-sectors to 12 (magenta) results in a better mean value at the cost of an edge throughput reduction due to the stronger interference in the edge regions. In summary, for a system based on 12 pairs of cross-polarized antenna elements 6 hard-sectorized sites is the most favorable configuration. Soft-sectorized networks with 9 and 12 cells per site perform slightly better or similar to that of conventional tri-sector network applying Rel. 10 MU-MIMO.

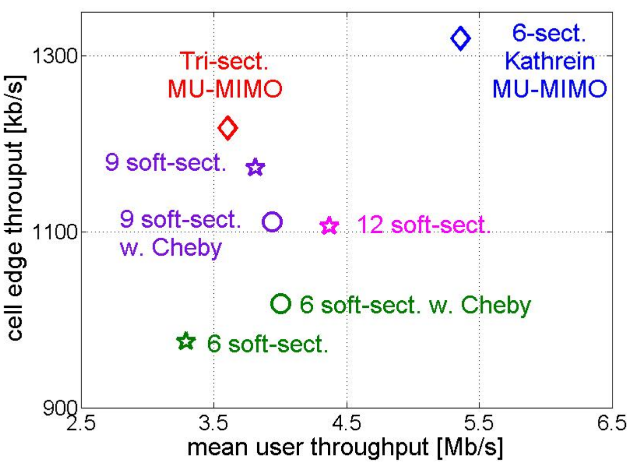

Figure 10. Mean and edge user throughput for conventional tri-sector site network applying MU-MIMO (red diamond), 6 hard-sectorized (blue diamond), 6-soft sectorized network with and without Chebyshev taper (green circle and star), 9-soft-sectorized network with (purple circle) and without taper (purple) and 12 soft-sectorized network (margenta star). The performance of the 3 last cases are quite similar. A loss in the edge user throughput can be charged up with a gain in the mean user throughput by tuning the fairness parameter of the PF scheduler.

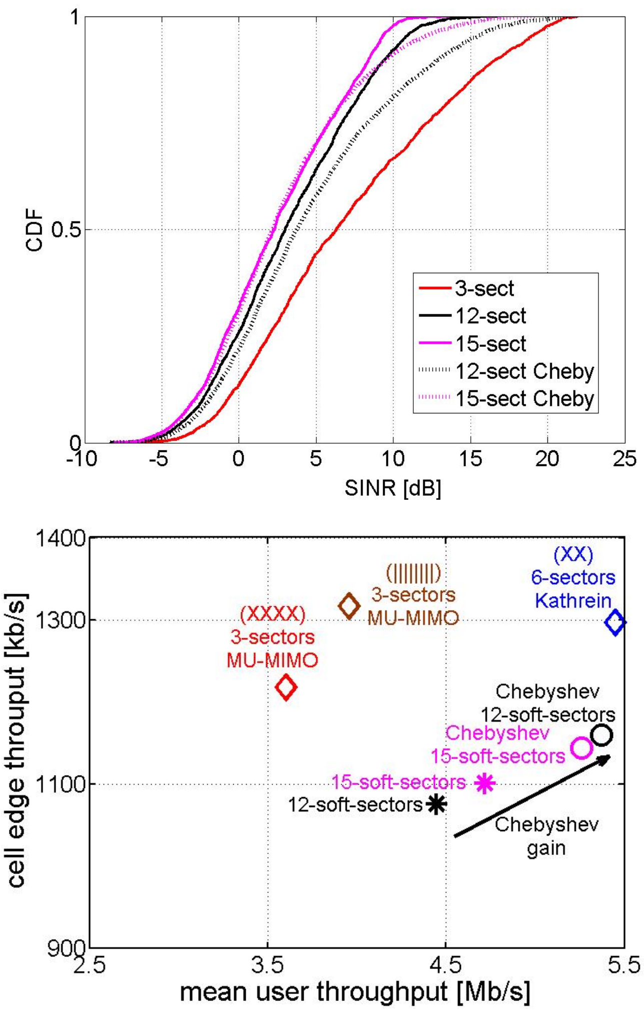

Figure 11. Soft-sectorization using an 8Tx co-polarized antennas, with and w/o Chebyshev tapering. Top: wideband SINR distributions for a tri-hard-sectorized (red), 12 soft-sectorized (black), 15 soft-sectorized (magenta) networks. Dotted and solid curves indicate the performance with and w/o tapering, respectively. Bottom: corresponding mean and edge user throughput.

2) Co-polarized antenna array (||||||||) *:* Sectorization gain ideally scales with the number of sub-divided sectors. The narrower the beamwidth the more soft-sector beams can be accomodated in a conventional hard-sector. Since the beamwidth is inversely proportional to the array aperture, the co-polarized antenna configuration allows to form narrower (to about 12°) beamwidth than the corresponding cross-polarized counterpart. As already discussed in section IV-B the number of different polarizations define the number of virtual transmit antenna element at the soft-sectors. In case of co-polarized based systems the created soft-sectors therefore transmit with a single virtual antenna element.

The sharp beams formed by an 8 antenna array exhibits steep rolloff sidewards, hence creates a more favorable conditions for the trade-off between interference due to soft-sector overlapping and better angular coverage. Figure 11 shows in the upper plot the wideband SINR distribution and in the lower plot the mean and edge user throughput for various network configurations based on a co-polarized system, including the use of Chebyshev filter. Keep the beamwidth constant so the higher the sectorization order, the more overlapping regions are created. The SINR distribution is pushed to a lower region with increasing sectorization order. On the other hand a higher order means a better spatial spectrum usage and a better system throughput. Since in the co-polarized configuration the soft-sectors transmit with a single virtual antenna element the gain in the SINR can directly be translated in system throughput improvement. This can be obeserved in the lower plot of figure 11. The user throughput gain increases with increasing number of soft-sectors (c.f. black and magenta symbols). This reflects the fact that the gain harvested from higher order sectorization offsets the increasing interference due to soft-sector overlapping. Applying Chebyshev filter pushes the entire SINR distribution to the higher region (c.f. solid and dotted black in upper plot of figure 11) for the 12 soft-sectors configuration and in the higher SINR range for the case of 15 soft-sectors. This leads to a large and moderate throughput improvement in mean and edge user throughput for the corresponding configuration. In short among different soft-sectorized configurations the 12 soft-sectors in combination with a Chebyshev window shows the best performance. Compared to a conventional tri-sectorized network applying MU-MIMO the soft-sectorized network achieves better performance but is still inferior the performance of a hard-sectorized network.

Table III summarizes the performance gain for all the investigated HOS configurations w.r.t. conventional tri-sector site networks. For the comparison the reference networks are equipped with antenna elements of the same polarization and apply Release 10 SU-/MU-MIMO. The case of 6 hard-sectorized network using 4 co-polarized antenna elements per sector is of little interest due to its very large physical dimension, thus is unlikely to be deployed in a practical field (s. also IV-C below).

Gain w.r.t. conv. tri-sect. MU-MIMO	mean user throughput [%]	edge user throughput [%]
X-polarized		
6 hard-sectors	51	6
6 soft-sectors	-9	-20
6 soft-sectors Cheby	11	-16
9 soft-sectors	6	-4
9 soft-sectors Cheby	9	-8
12 soft-sectors	10	-14
Co-polarized		
12 soft-sectors	12	-18
12-soft sectorsCheby	36	-12
15 soft-sectors	19	-16
15 soft-sectors Cheby	33	-13

Table III

PERFORMANCE GAIN OF DIFFERENT NETWORK CONFIGURATIONS W.R.T. CONVENTIONAL TRI-SECTOR SITE NETWORK.

C. Implementation issues

Despite the higher expected gain in HOS up to now it is seldom observed in the field. The reason for that is the feasibility for the implementation. Antennas with narrower beamwidth needed of 6 hard-sectorized network is double as large as a panel of a conventional tri-sectorized network. The big antenna panels lead to stronger wind loading, higher torque and montage issues. Further the lower public acceptance causes difficulties in getting deployment permission from regulatory authority and higher siting and zoning costs. There are a lot of efforts from antenna manufacturer side (like Kathrein and Comscope) to facilitate 6 sector site deployment. As an example the intergration of 2 separate beams functionality in a single panel (housing), the so-called dual or twin beams antennas. The advantages here are the slightly more compact physical size of the panel and an easier montage, calibration, synchronization as well as maintenance procedures. Compared to hard-sectorized configuration the soft-sectorization exhibits smaller physical size (also due to the required smaller inter-antenna elements). There are several advantages deploying soft-sectorization. A soft-sectorized network operates either with 2 or single virtual antenna elements. This deceases the CQI feedback load in the uplink and simplifies downlink scheduler and control signals.

V. CONCLUSION

System perfomance comparisons between conventional tri-sectorized networks with 8Tx antenna elements per cell, deploying release 10 CL-MIMO transmission techniques and higher order sectorizied networks have been carried out. Numerical simulation results show advantages in deploying HOS configurations in both complexity reduction (single Tx transmission) and capacity improvement. Hard-sectorized networks exhibit the highest performance, provided antennas with suitable characteristics are available. Using the throughput of a conventional tri-sectorized network applying Rel. 10 CL-MU-MIMO as base line, the gain in deploying hard-sectorized networks amount to 51% and 6% in mean and edge user throughput, respectively. Soft-sectorization based on cross-polarized antennas shows a slightly better performance. A gain between (6-10)% in mean is achieved at the expense of a loss of (4-14)% in cell edge user throughput. Soft-sectorization based on co-polarized antennas results in a higher HOS gain exploitation, up to 36% improvement in mean against a loss of 12% in edge user throughput can be achieved. It was shown that the performance of soft-sectorized system, in particular the edge user throughput, is sensitive to the sector beam shaping and therefore to the antenna characteristic of the deployed antennas. Careful filter design is needed to harvest the achievable soft HOS gain.

REFERENCES

[1] H. Holma, A. Toskala, WCDMA for UMTS Radio access for third generation mobile communication, 2010

[2] T. Baumgartner, E. Bonek, On the optimum number of beams for fixed beams smart antennas in UMTS FDD, IEEE Trans. on wireless communications, Vol. 5, No. 1, Jan. 2006

[3] A. Osseiran and A. Logothetis, A WCDMA Radio Network System: Modeling and Evaluations”, IEEE Trans. Ant. Propag., Vol. 54, p. 3302-3316, Nov. 2006

[4] Fredrik Athley, Martin N. Johansson, and Andreas Nilsson, ”Increased sectorization: Horizontal or vertical? ”, Proceeding Vehicular Technology Conference (VTC Fall), 2013 IEEE 78th; January 2013

[5] H. Huang, O. Alrabadi, J. Daly, D. Samardzija, C. Tran, R. Valenzuela, S. Walker, ”Increasing throughput in cellular networks with higher-order sectorization”, Proceeding Asilomar Conference 2010, 630-635, Nov. 2010

[6] 3GPP TR 36.814 Release 9 2 V9.0.0 (2010-03)

[7] 3GPP TSG RAN WG1 N 72bis Chicago, USA, 15th-19th April 2013, R1-131761

[8] Mirette Sadek, Alireza Tarighat, Ali H. Sayed, ”A Leakage-Based Precoding Scheme for Downlink Multi-User MIMO Channels”, IEEE Trans. on Wireless Communications, Vol. 6, No. 5, May 2007

[9] T. Yoo and A. Goldsmith, ”On the optimality of multiantenna broadcast scheduling using zero-forcing beamforming” Vol. 24, No. 3, pp. 528 541, Mar. 2006.

[10] Matteo Trivellato, Federico Boccardi, and Howard Huang, ”On Transceiver Design and Channel Quantization for Downlink Multiuser MIMO Systems with Limited Feedback”, IEEE Journal on selected Areas in Communications, Vol. 26, NO. 8, Oct.2008

[11] http://www.kathrein.de/mobilfunk/produktuebersicht

[12] M. U. Sheikh, J. Lempiainen, H. Ahnlund, ”Advanced antenna techniques and higher order sectorization with novel network tessellation for enhancing macro cell capacity in DC-HSDPA network”, International Journal of Wireless Mobile Networks, Oct. 2013, Vol. 5, No. 5